Front. Earth Sci. 2025, 19(2): 261–274
https://doi.org/10.1007/s11707-024-1140-z

RESEARCH ARTICLE

Cretaceous provenance changes in the Yishu Rift Basin, east China: implications for the uplift of East Asian coastal mountains

Jiazhen XIANG[1], Xue GU[1], Shuo CAO[1,2], Laiming ZHANG (✉)[1,2,3], Peng CHEN[1], Chengshan WANG[1,2,3]

1 School of the Earth Science and Resources, China University of Geosciences, Beijing 100083, China
2 Frontiers Science Center for Deep–time Digital Earth, China University of Geosciences, Beijing 100083, China
3 State Key Laboratory of Geomicrobiology and Environmental Changes, China University of Geosciences, Beijing 100083, China

Abstract An early Late Cretaceous NW-SE compressional event that induced the uplift of the coastal mountains was recognized among the overall extensional regime in east China. While previous studies have explored the paleoelevation, paleogeographical extent, and possible climatic effects of coastal mountains, the exact timing of initial uplift has remained elusive. In this study, we applied detrital zircon U-Pb geochronology to sandstones from the Dasheng Group in the Yishu Rift Basin, east China. Our results suggest that the primary provenance of the Dasheng Group is intermediate-basic volcanic rocks (800–500 Ma, 330–215 Ma, and 150–122 Ma) derived from the Luxi Uplift and Sulu Orogenic Belt, and the secondary provenance is Mesoproterozoic-Paleozoic metamorphic rocks (2500–2300 Ma and 1850–1600 Ma) derived from the Jiaobei Terrane. The zircon age peaks of the Dasheng Group in the Yishu Rift Basin are nearly the same as those of the Lower Cretaceous Laiyang Group in the Jiaolai Basin. However, the proportion of pre-Mesozoic zircons decreases. For the Mesozoic zircons, although their main age peak is close to that of the Laiyang Group, their secondary age peak is similar to that of the Wangshi Group. We infer that the transitional characteristic of the Dasheng Group was caused by the initial uplift of the coastal mountains. Therefore, we speculate that the initial uplift of the coastal mountains occurred during the deposition of the Dasheng Group, and limit the maximum depositional age (MDA) of the Dasheng Group to 100–95 Ma.

Keywords Dasheng Group, Yishu Rift Basin, Jiaolai Basin, detrital zircon U-Pb geochronology, provenance analysis

Received August 22, 2024; accepted December 4, 2024

E-mail: lzhang@cugb.edu.cn

1 Introduction

In contrast to the landscape of “high elevation in west China and low elevation in east China” at present, the landscape was “high elevation in east China and low elevation in west China” at the end of the Cretaceous (Wang, 1998 and 2004). The Cretaceous was a transitional period from “east-high-west-low” to “east-low-west-high,” with widespresd uplift of the coastal mountains in East China (Chen, 1997; Zhang et al., 2016; Suo et al., 2019; Liu et al., 2024). These mountains blocked moisture from paleo-Pacific region and led to arid-semiarid climates, vast rain shadows, and the development of “intermountain ergs” in the hinterlands of east China (Jiang et al., 2006; Cao et al., 2020; Zhang et al., 2021b; Wu et al., 2022; Cao et al., 2023). Therefore, investigating the evolution of coastal mountains, which could help to shed new light on the Cretaceous terrestrial climate in east China, is critical.

Chen (1997) first proposed that coastal mountains were 3500–4000 m in height and 500 km in width during the Late Cretaceous on the basis of the widely distributed molasses along Fujian and Zhejiang Provinces in south-east China. Since then, many studies have explored the paleoelevation (Zhang et al., 2016), paleogeographical extent (Yan et al., 2011; Hu et al., 2012; Tan et al., 2020), and possible climatic effects of coastal mountains (Cao et al., 2020, 2023; Zhang et al., 2021b). Recently, on the basis of the provenance change between the Lower Cretaceous Laiyang Group and Upper Cretaceous Wangshi Group in the Jiaolai Basin, previous studies reported that the initial uplift of the coastal mountain occurred ~85 Ma (Tan et al., 2020; Zhang et al., 2021a). However, the exact age is not well constrained due to the lack of sedimentary strata between the Laiyang and Wangshi groups in the Jiaolai Basin, east China.

In this study, we investigate the Lower Cretaceous

Dasheng Group in the Yishu Rift Basin, which lies adjacent to the Jiaolai Basin (Fig. 1). Zircon U-Pb geochronological analyses were applied to sandstones from the Dasheng Group to reconstruct the provenance history of the Yishu Rift Basin during the Cretaceous. The Dasheng Group is temporally equivalent to the late Early Cretaceous to the early Late Cretaceous Qingshan Group volcanic rocks in the Jiaolai Basin (Li and Zhao, 1992; Liu et al., 2003). Therefore, the provenance changes in the Dasheng Group and the Cretaceous paleogeographic evolution of the Yishu Rift Basin could help to further constrain the initial uplift of coastal mountains.

2 Geological setting

2.1 Jiaolai Basin

The Jiaolai Basin, located in Shandong Province (Fig. 1), is a typical Cretaceous terrestrial volcano-sedimentary basin (Zhang et al., 2019, 2021a; Tan et al., 2020). It lies adjacent to the Tanlu Faults to the west, overlaps with the Jiaobei Terrane to the north, and connects with the Sulu Orogenic Belt to the east. In the Jiaolai Basin, the Cretaceous strata include the Laiyang Group, Qingshan Group, and Wangshi Group (Fig. 2) (Zhang et al., 2019, 2021a; Tan et al., 2020).

The Lower Cretaceous Laiyang Group is composed of purple-red sandstones, gray-green mudstones, and calcareous sandstones, with occasional volcanic interlayers. It comprises the Wawukuang, Linsishan, Zhifengzhuang, Shuinan, Longwangzhuang, and Qugezhuang Formations, from bottom to top (Tan et al., 2020). On the basis of isotopic data from the volcanic rocks ($^{40}Ar/^{39}Ar$ and SHRIMP U-Pb), Zhang et al. (2008) constrained the bottom of Laiyang Group to be 131 Ma in age. Zhang et al. (2019) constrained the uppermost Laiyang Group to be ~114 Ma in age on the basis of the

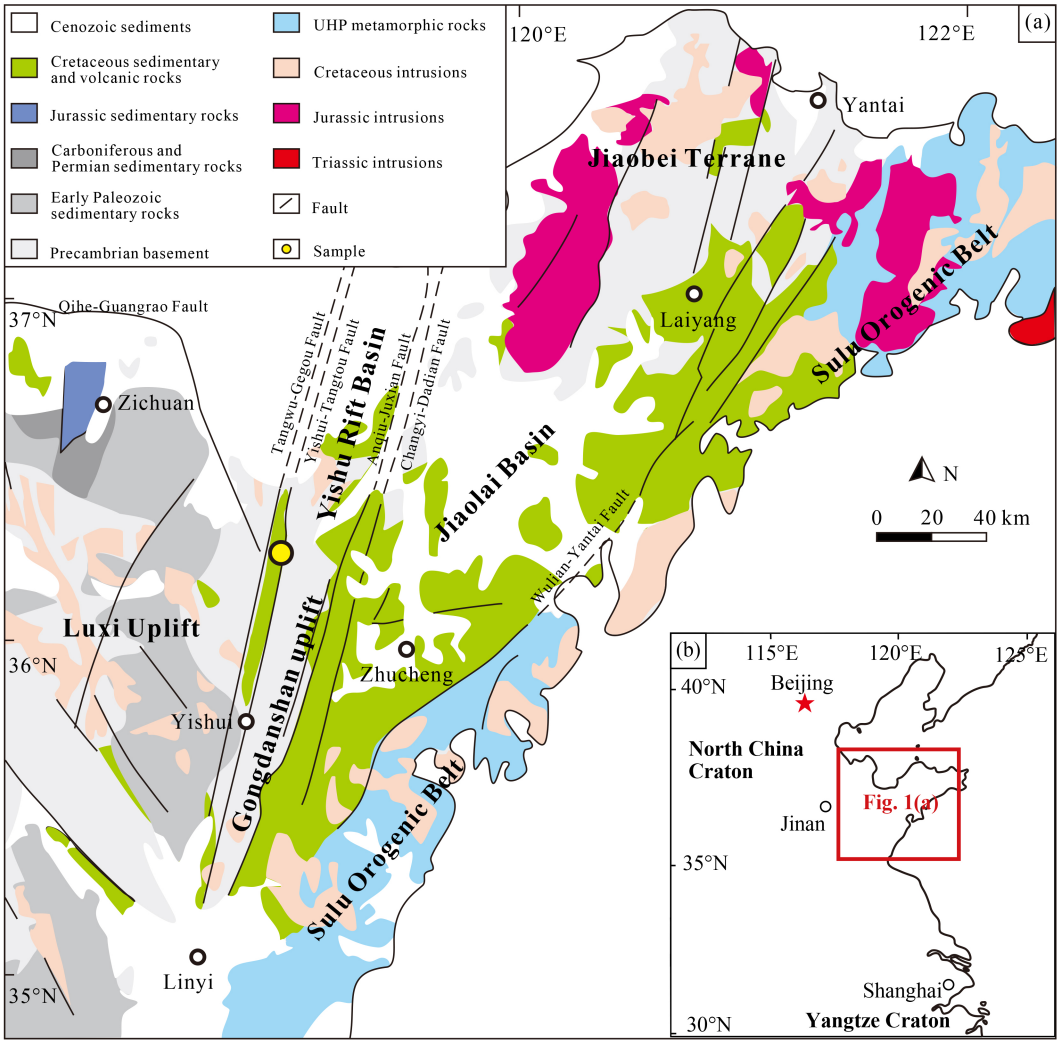

Fig. 1 Geological setting of the Yishu Rift Basin. (a) Schematic geological map of the Jiaolai Basin and Yishu Rift Basin, modified after Xu et al. (2012). The yellow circles are sampling points; (b) Major tectonic units in East China, modified after Luo et al. (2018) and Yang et al. (2020).

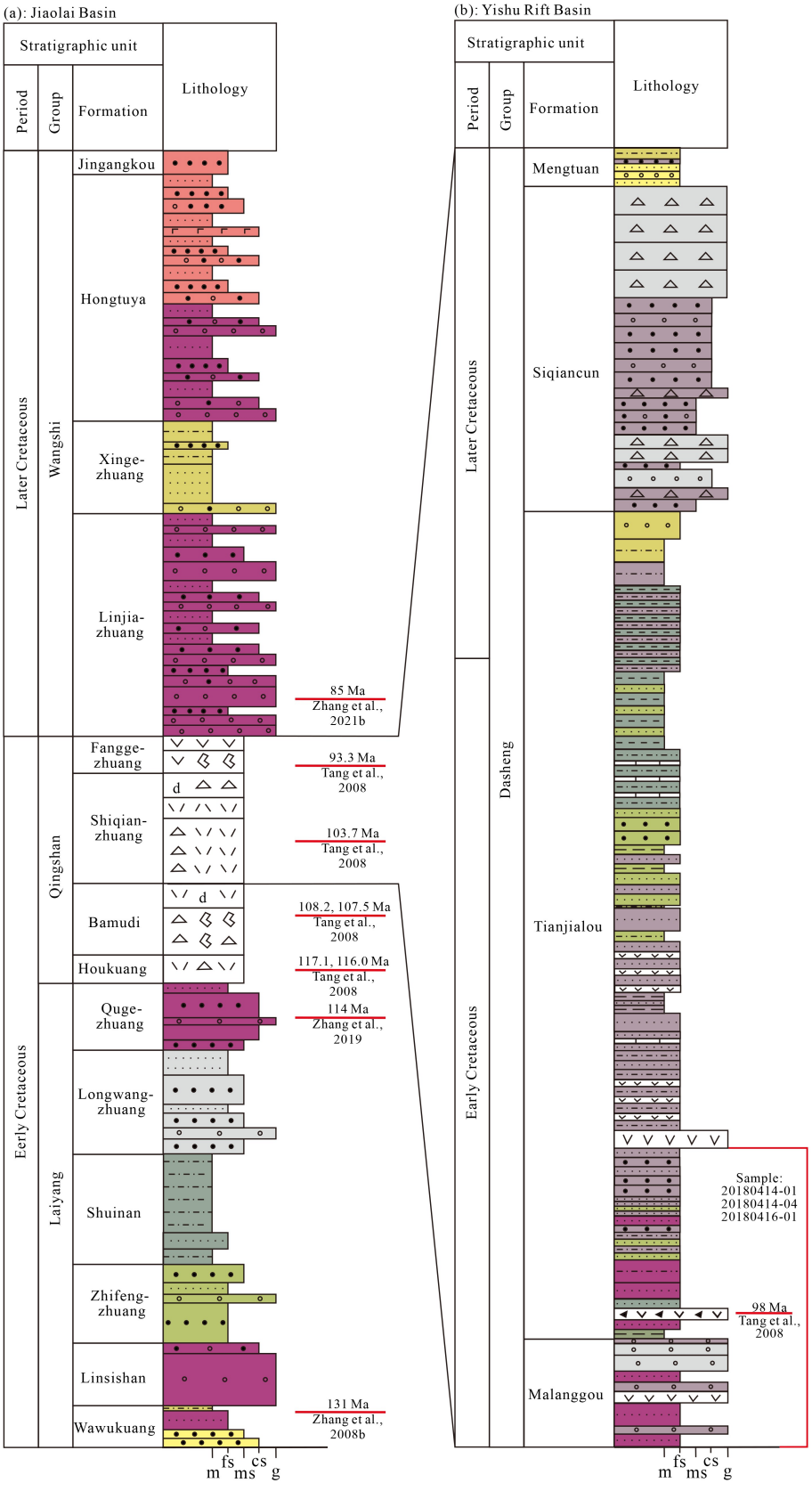

Fig. 2 Cretaceous stratigraphy of the (a) Jiaolai Basin and (b) Yishu Rift Basin. Modified after Si (2002), Liu et al. (2003), Zhang et al. (2019), and Tan et al. (2020).

youngest U-Pb zircon ages from the Qugezhuang Formation. Therefore, the sedimentary age of the Laiyang Group is ~130–115 Ma.

Above the Laiyang Group, the Lower Cretaceous Qingshan Group consists of volcanic and sedimentary rocks. From bottom to top, it is subdivided into the Houkuang, Bamudi, Shiqianzhuang, and Fanggezhuang Formations (Tan et al., 2020). Tang et al. (2008) collected samples from the Qingshan Group and obtained relatively reliable ages for the volcanic rocks, including 117.1 Ma and 116.0 Ma for the Houkuang Formation, 108.2 Ma and 107.5 Ma for the Bamudi Formation, 103.7 Ma for the Shiqianzhuang Formation, and 93.3 Ma for the Fanggezhuang Formation. Therefore, the magmatic events of the Qingshan Group occurred at 120–90 Ma.

The Upper Cretaceous Wangshi Group unconformably overlies the Qingshan Group. From bottom to top, it is composed of the Linjiazhuang, Xingezhuang, Hongtuya, and Jingangkou Formations (Zhang and Dong, 2008; Tan et al., 2020). It is characterized by fluvial purple–red sandstones interbedded with conglomerates, minor mudstones and calcareous nodules (Tan et al., 2020). A previous study suggested that the Linjiazhuang Formation at the bottom of the Wangshi Group began to be deposited at 85 Ma (Zhang et al., 2021a).

Zhang et al. (2016) suggested that the uplift of coastal mountains during the late Early Cretaceous to early Late Cretaceous transformed the Jiaolai Basin into an intermontane basin (Zhang et al., 2016). The Laiyang Group received sediments from the relatively distal Sulu orogenic belt and Jiaobei Terrane granitic and metamorphic rocks during the Early Cretaceous before 114 Ma (Zhang et al., 2019; Tan et al., 2020). However, during the Late Cretaceous (after 85 Ma), the uplift of the coastal mountains blocked the ancient materials from the Sulu Orogenic Belt and Jiaobei Terrane, and almost all the zircon U-Pb ages were Mesozoic in age, which implies that the provenance of the Wangshi Group shifted to Mesozoic intrabasinal basic–intermediate volcanic rocks (i.e., Qingshan Group) (Zhang et al., 2008; Tan et al., 2020; Zhang et al., 2021b). During the late stage, the provenance changed to a multimember mixed source, including the Sulu Orogenic Belt, Jiaobei Terrane, and Qingshan Group, with a gradual decrease in the proportion of the Qingshan Group (Zhang et al., 2021b).

2.2 Yishu Rift Basin

In the western part of the Jiaodong Peninsula, east China, the Yishu Fault Zone extends from the Tanlu Fault (Fig. 1). From east to west, it contains the Changyi-Dadian Fault, Anqiu-Juxian Fault, Yishui-Tangtou Fault, and Tangwu-Gegou Fault (Zhang and Dong, 2008; Luo et al., 2018).

The Yishu Rift Basin is a sedimentary basin within the Yishu Fault Zone. In this basin, the Cretaceous alluvial-fluvial mixture is named the Dasheng Group. It can be subdivided into the Malanggou, Tianjialou, Siqiancun, and Mengtuan Formations (Fig. 2). The Malanggou Formation comprises purple and gray-purple coarse sandstones and conglomerates with thin layers of siltstones. The Tianjialou Formation comprises yellow-green sandstones and argillaceous siltstones. The Siqiancun Formation consists of gray-purple siltstones and conglomerates. The Mengtuan Formation consists of gray-purple-yellow siltstones and argillaceous sandstones (Li and Zhao, 1992; Si, 2002). Previous studies have suggested that the Dasheng Group is temporally equivalent to the Qingshan Group in the adjacent Jiaolai Basin in terms of stratigraphic lithology and palynomorphs (Li and Zhao, 1992; Si, 2002; Liu et al., 2003). The zircon U-Pb age of the andesite in the Tianjialou Formation is 95 Ma (Tang et al., 2008), which corresponds to the middle-upper part of the Qingshan Group (i.e., the Shiqianzhuang Formation and Fanggezhuang Formation) and confirms the above conclusion.

2.3 Jiaobei Terrane, Sulu Orogenic Belt, and Luxi Uplift

The Jiaobei Terrane is located north-east of the Jiaodong Peninsula, and formed at ~1.9 Ga (Fig. 1). It is bounded by the Wulian-Yantai Fault to the south-east and the Yishu Fault to the north-west (Zhao et al., 2016). The Jiaodong Group experienced two metamorphic events (~2.5 Ga and ~1.85–1.95 Ga) and three magmatic events (~2.9 Ga, ~2.7 Ga, and ~2.5 Ga) (Liu et al., 2012, 2013a; Wu et al., 2014; Zhao et al., 2016). The detrital zircon U-Pb ages of the Penglai Group are 2.45–2.1 Ga and 2.0–1.7 Ga (Li et al., 2007; Zhou et al., 2008; Liu et al., 2013b). The metamorphic events of the Fenzishan and Jingshan Groups occurred at 1.95–1.80 Ga (Tang et al., 2007; Liu et al., 2012, 2013b). In addition, the Jiaobei Terrane experienced two Mesozoic magmatic events at 160–150 Ma and 130–110 Ma (Liu et al., 2011).

The Sulu Orogenic Belt is located in the southern Jiaodong Peninsula and adjacent to the North China Block, which is separated by the north-east-trending Wulian-Yantai Fault (Wu and Zheng, 2013; Zhao et al., 2016). The Mesozoic igneous rocks in the Sulu Orogenic Belt experienced three metamorphic events (246–244 Ma, 235–225 Ma, and 215–208 Ma) and two magmatic events (160–150 Ma and 130–110 Ma) (Zhou et al., 2008; Zhang et al., 2010). The zircon ages of the Sulu Orogenic Belt are primarly 800–500 Ma and 2.05–1.85 Ga (Zhang et al., 2010).

The Luxi Uplift is located in the south-eastern part of North China (Fig. 1) and is bounded by the Qihe-Guangrao Fault Zone to the north, the Liaocheng-Lankao Fault Zone to the west, and the Yishu Fault Zone to the east (Li et al., 2005; Guo, 2014). The age of the Archean granite–greenstone belt ranges from 2.75 Ga to 2.5 Ga. The Paleoproterozoic orogenic granite rocks include two stages of basic dike swarms with zircon ages of 1.8 Ga

and ~1.5 Ga (Hou et al., 2005; Hu et al., 2009; Xu et al., 2012). During the Mesozoic, the sedimentary cover was intruded by gabbroic granodioritic, and granitic rocks at 177–160 Ma and 150–100 Ma (Song and Li, 2001; Li et al., 2005; Guo, 2014).

3 Samples and methods

3.1 Samples

Our samples were collected from the standard profile of the Dasheng Group in Dasheng town, Anqiu City (Fig. 1). The section lies between Dingjiagou Village and Siqian Village (36.3°N, 118.9°E) and exposes the Malanggou, Tianjialou, and Siqiancun Formations. The Malanggou Formation is characterized by gray conglomerates and purplish red tuffs. The Tianjialou Formation consists of purple red and purple-gray fine sandstones and mudstones, as well as yellow-green fine sandstones, siltstones, and mudstones. The Siqiancun Formation consists of purple-red and purple-gray sandstones with a few breccias. In this study, three sandstones were collected for zircon U-Pb age analysis.

3.2 Methods

The zircon U-Pb ages were analyzed via LA-ICP-MS laser ablation analysis at Wuhan Shangpu Analysis Technology Co., Ltd. The analytical process involved the following steps. 1) The original rock samples were organized and crushed into small pieces. Zircon single minerals were selected according to conventional gravity and magnetic separation, and zircon single mineral particles were manually selected under a binocular lens. Zircon cathodoluminescence, transmitted light, and reflected light were placed in epoxy resin for subsequent analysis. Relatively complete zircon particles were selected by comparing the cathodoluminescence image and the transmittance reflection image in order, and the measurement was completed via a Laura mass spectrometer (Woodhead et al., 2004, 2007). 2) The data were calibrated via ICPMSDataCal software (Liu et al., 2010a, 2010b), and two 91500 standard points were measured for every five sample points. The U–Th Pb isotope ratio standards for zircon standard 91500 described by Wiedenbeck (1995) were followed. 3) The data were imported into Isoplot/Ex_Ver3 software (Torres et al., 2012) to generate age distribution harmonics and histograms. When the covariance plots are created, zircon data that deviated significantly from the covariance line and had a covariance error greater than 0.1 were excluded. For the age histogram, the $^{206}Pb/^{238}U$ isotope ages for zircons younger than 1000 Ma and the $^{206}Pb/^{207}Pb$ isotope ages for zircons older than 1000 Ma were used.

4 Results

4.1 Zircon CL images

Cathodoluminescence (CL) images reflect trace element variations (e.g., U, Y, Dy, and Tb) on the surface of zircons and/or lattice defects (Li, 2009). Trace elements are often unevenly distributed, resulting in oscillatory zoning (Hoskin and Schaltegger, 2003). By analyzing CL images, combined with Th/U ratios, the sources of zircons can be distinguished. The Th/U ratios of magmatic zircons are related to the Th and U contents in magmas and their distribution coefficients between zircons and magmas (Geisler et al., 2001, 2003; Li, 2009), and the corresponding relationship is as follows:

$$(\mathrm{Th/U})_{\mathrm{zircon}} \approx (D^{\mathrm{Th}}/D^{\mathrm{U}})_{\mathrm{zircon/melt}} \times (\mathrm{Th/U})_{\mathrm{melt}}, \quad (1)$$

in general, when $(D^{\mathrm{Th}}/D^{\mathrm{U}})_{\mathrm{zircon/melt}} \approx 0.2$, the average Th/U ratio in crustal material is approximately 4, so the Th/U ratio of magmatic zircon is usually close to 1 and generally > 0.4 (Hermann et al., 2001). Since Th^{4+} has a larger ionic radius than does U^{4+}, Th is more unstable than is U in the zircon lattice, and Th is more likely to be expelled from the zircon lattice than is U during metamorphic recrystallization, resulting in a relatively low Th/U ratio in the region of recrystallized metamorphic zircon. Generally, a greater degree of metamorphic recrystallization is associated with a lower Th/U ratio of the metamorphic recrystallized zircon crystal domain, which is usually < 0.1 (Kerrich and King, 1993; Pidgeon et al., 1998).

Magmatic zircons typically exhibit euhedral to hypidiomorphic columnar shapes with sharp crystal edges, internal oscillatory zoning, bright CL, and high Th/U ratios (> 0.4). The metamorphic zircons are mostly rounded or irregular with smooth crystal edges and complex crystal faces with dissolution, lack zoning and CL, and exhibit low Th/U ratios (< 0.1). The hydrothermal zircons are generally irregular, lack clear prismatic edges, zoning, and CL, and possess very high Th/U ratios.

In this study, the Paleoproterozoic to Archean zircons (3.0–1.6 Ga) mostly display rounded shapes with smooth edges (Fig. 3) and relatively low Th/U ratios, suggesting metamorphic origins. The Mesozoic zircons (130–110 Ma) mostly appear in tabular structures with indistinct oscillatory zones (Fig. 3), suggesting a mid- to basic volcanic origin (Hoskin and Schaltegger, 2003; Wu et al., 2004).

4.2 Zircon U-Pb ages

4.2.1 Sample 20180414-01

Among the 100 analyses, 97 provided concordant ages

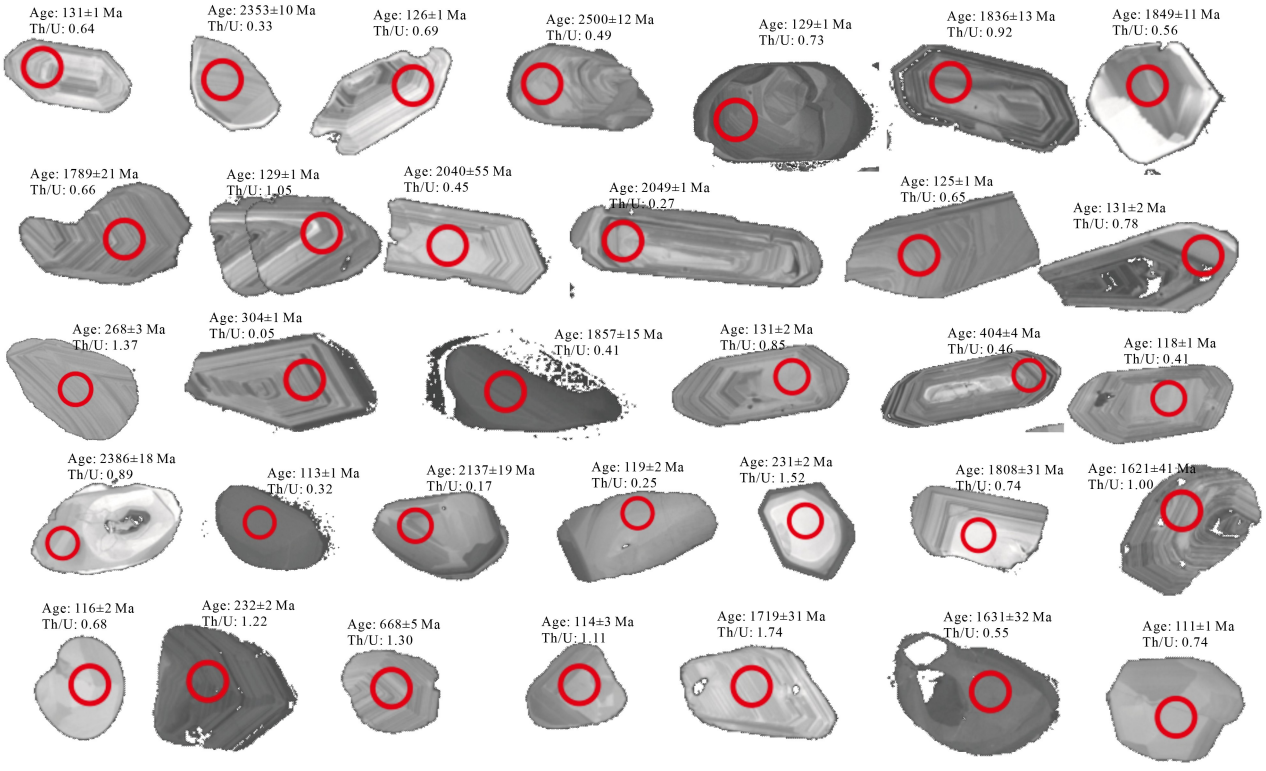

Fig. 3 The representative zircon CL images of the Dasheng Group.

ranging from 2711 to 122 Ma (Figs. 4(a) and 4(b)). The data include 40 zircons aged in the Mesozoic, 8 in the Paleozoic, 3 in the Middle-Neoproterozoic, and 46 in the Early-Proterozoic–Archean. The ages exhibit four major populations at 2500–2250 Ma, 2000–1500 Ma, 320–247 Ma, and 133–110 Ma, with minor peaks at 250 Ma and ~130 Ma.

4.2.2 Sample 20180414-04

Among the 100 analyses, 96 provided concordant ages ranging from 2554 Ma to 97 Ma (Figs. 4(d) and 4(d)). The data include 34 zircons aged in the Mesozoic, 10 in the Paleozoic, 2 in the Middle-Neoproterozoic, and 51 in the Early-Proterozoic–Archean. The ages exhibit four major populations at 2600–2250 Ma, 2000–1500 Ma, 320–245 Ma, and 130–100 Ma, with minor peaks at 270 Ma and ~130 Ma.

4.2.3 Sample 20180416-01

Among the 100 analyses, 87 provided concordant ages ranging from 2169 Ma to 112 Ma (Figs. 4(e) and 4(f)). The data include 16 zircons aged in the Mesozoic, 18 in the Paleozoic, 30 in the Middle-Neoproterozoic, and 23 in the Early-Proterozoic–Archean. The ages exhibit four major populations at 2000–1700 Ma, 1150–800 Ma, 700–400 Ma, 300–200 Ma, and 135–110 Ma, with minor peaks at 500 Ma and ~130 Ma.

In total, 300 sets of U-Pb ages were obtained, with 280 sets providing concordant ages (Fig. 5). The zircon ages range from 2711 Ma to 97 Ma, including 90 ages in the Mesozoic, 32 in the Paleozoic, 37 in the Meso-Neoproterozoic, and 121 in the Early Proterozoic–Archean. The age peaks include 2500–2300 Ma, 1,850–1600 Ma, 800–500 Ma, 330–215 Ma, and 150–122 Ma. The highest peak occurred at 150–122 Ma, followed by 1850–1600 Ma.

5 Discussions

5.1 Provenance of the Dasheng Group

A previous study suggested that the sandstone clasts (mainly quartz and feldspar) from the bottom of the Dasheng Group (i.e., Malanggou Formation) are predominantly felsic volcanic rocks (Song, 2020). The alteration of these clasts is minimal, and the quartz is poorly pure. Song (2020) suggested that the zircon U-Pb ages of the Malanggou Formation show a main peak at 141–117 Ma and a secondary peak at 1852–499 Ma, which suggests that the provenance was mainly from the Luxi Uplift and the intrabasinal Gongdan Mountain Uplift, with no contribution from the Sulu Orogenic Belt (Song, 2020). Additionally, the measurements of trough cross-bedding and imbricate gravels in the Dasheng Group indicate NW and NE flow directions (Yu et al., 2003), which suggests that the western part of the Luxi Uplift provided the provenance for the Malanggou

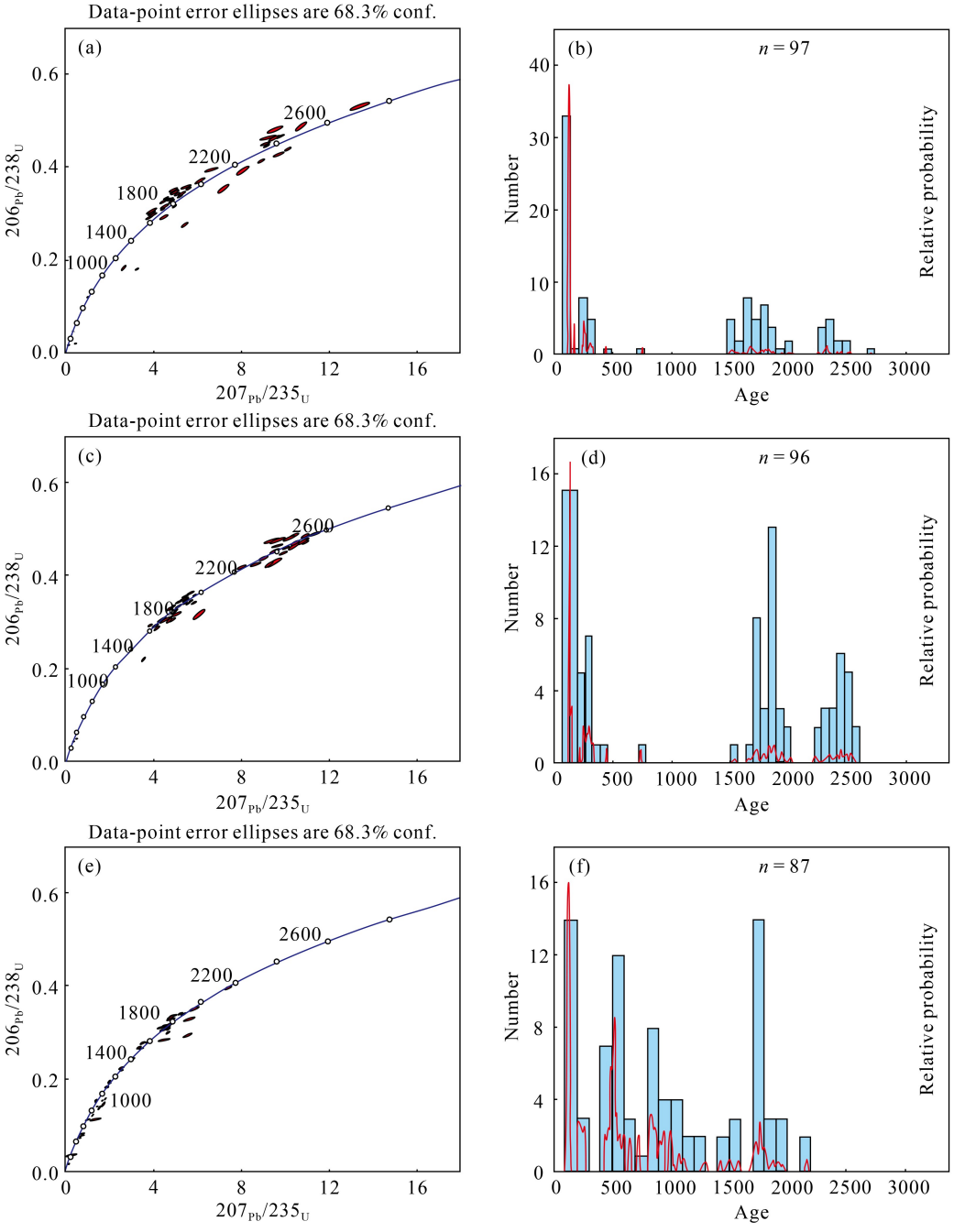

Fig. 4 The concordia plots (a, e, and e) and the probability density (b, d, and f) for detrital zircon U-Pb ages of samples 20180414-01 (a and b), 20180414-04 (c and d), and 20180416-01 (e and f).

Formation and ruled out the Jiaobei Terrane.

As mentioned above, in this study, the zircon age peaks are 2500–2300 Ma, 1850–1600 Ma, 800–500 Ma, 330–215 Ma, and 150–122 Ma for the Dasheng Group (Fig. 5). Notably, we recognized a zircon age peak at 800–500 Ma, which was never recognized by Song (2020) studies (Fig. 5). We attribute this phenomenon to the provenance of the Sulu Orogenic Belt (Zhang et al., 2019, 2021a; Tan et al., 2020). Moreover, the age peak at 1850–1600 Ma may also indicate provenance from the Jiaobei Terrane. Since the zircon age peak from the Yangtze Block (i.e., 2000 Ma) is slightly older than that from the Dasheng Group (i.e., 1850–1600 Ga), we suggest that the Yangtze Block did not provide provenance to the Dasheng Group.

Our study is also supported by previous studies based on paleocurrent and heavy mineral analyses (Yu et al., 2003; Bu et al., 2012). As mentioned above, the paleocurrent reconstructions of the Tianjialou and Siqiancun Formations indicate NW and NE flow directions (Yu et al., 2003). According to the flow directions, the potential source areas were the Luxi Uplift,

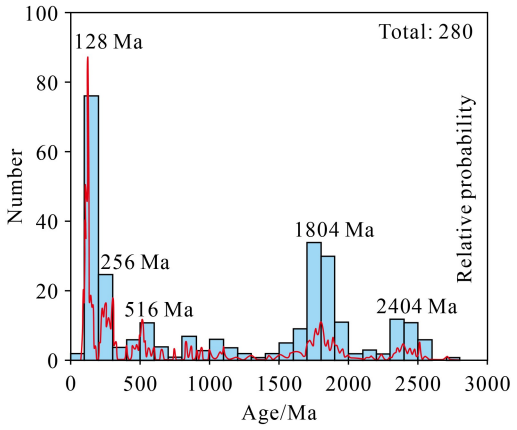

Fig. 5 The plot of the probability density for detrital zircon U-Pb ages of the Dasheng Group.

the intrabasinal Gongdan Mountain Uplift, and the extrabasinal Sulu Orogenic Belt. In addition, the heavy mineral combinations reflect features of both the Luxi and Jiaodong metamorphic rocks, which proves that the main provenances of the Yishu Rift Basin were the Luxi Uplift and Jiaodong areas (e.g., Jiaobei Terrane and Sulu Orogenic Belt) (Bu et al., 2012). In conclusion, we suggest that the source areas of the Dasheng Group in the Yishu Rift Basin were the Luxi Uplift, the Sulu Orogenic Belt, and the Jiaobei Terrane.

5.2 Provenances of the Yishu Rift Basin and the Jiaolai Basin

Separated by the Anqiu-Juxian Fault and Changyi-Dadian Fault, the Yishu Rift Basin and the Jiaolai Basin are not only geographically close to each other but also have similar sedimentary characteristics. A previous study suggested that the uplift of coastal mountains caused provenance changes between the Laiyang and Wangshi Groups in the Jiaolai Basin. The Dasheng Group in the Yishu Rift Basin is temporally equivalent to the Qingshan Group in the Jiaolai Basin; here, we compare the provenances of these two basins to further constrain the uplift of coastal mountains. Our results suggest that the provenance of the Dasheng Group in the Yishu Rift Basin has transitional characteristics from that of the Laiyang Group to that of the Wangshi Group in the Jiaolai Basin (Fig. 6).

First, the provenance of the Laiyang Group is primarily from the distal Sulu Orogenic Belt and the Jiaobei Terrane (Tan et al., 2020) (Fig. 6). The zircon-tourmaline-rutile (ZTR) ratio of the Laiyang Formation is between 8% and 44%, which also indicates long–distance transport (Morton and Hallsworth, 1994; Zhang et al., 2015). The provenance of the Wangshi Group is primarily the intrabasinal Qingshan Group (Tan et al., 2020). The ZTR of the Wangshi Group is ~6%–16%, which also indicates short-distance transport. With

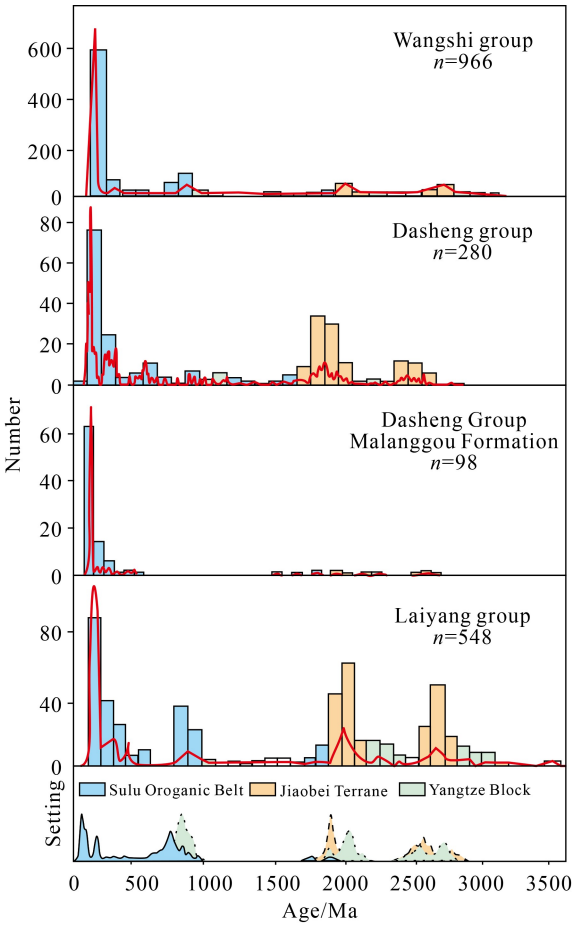

Fig. 6 The zircon age histograms of the major provenance setting of the Laiyang, Wangshi, and Dasheng groups. The data of the Laiyang and the Wangshi groups are derived from Tan et al. (2020). The data of the Malanggou Formation is derived from Song (2020). The data of the setting is derived from Liu (2018) and Zhang et al. (2019).

respect to the Yishu Rift Basin, our results suggest that the Dasheng Group has mixed provenances from the distal Luxi Uplift, Sulu Orogenic Belt, and Jiaobei Terrane, and intrabasinal Gongdan Mountain Uplift (Fig. 5).

Second, in the Yishu Rift Basin, the zircon U-Pb age distribution of the Dasheng Group is similar to that of the Laiyang Group in the Jiaolai Basin, specifically in that they both have secondary peaks at 2500–2300 Ma, 1850–1600 Ma, and 800–500 Ma. In addition, these two groups predominantly consist of intermediate-basic magmatic rocks, and their zircon CL images share the same features (Fig. 3). However, the percentages of the secondary peaks of the Dasheng Group are lower than those of the Laiyang Group, which is a typical characteristic of the Wangshi Group.

Third, for the Mesozoic zircon ages, the Laiyang Group ages range from 152–114 Ma with a peak at ~130 Ma, whereas the Wangshi Group ages range from 154–95 Ma with a peak at ~110 Ma (Fig. 7). With respect to the Yishu Rift Basin, the Mesozoic zircon ages of the

Dasheng Group range from 250–97 Ma, with a main peak at ~130 Ma and a secondary peak at ~110 Ma (Fig. 7). Therefore, the Mesozoic zircon ages distribution of the Dasheng Group reflects mixed provenance characteristics of both the Laiyang and Wangshi Groups in the Jiaolai Basin. Notably, we recognized a zircon age peak at 800–500 Ma, which is never recognized by Song (2020) (Fig. 5). Here we attribute it to the provenance of the Sulu Orogenic Belt (Zhang et al., 2019, 2021a; Tan et al., 2020). For the Dasheng Group, although its range of the Mesozoic zircon ages is similar to that of the Wangshi Group, the clear major peak at ~130 Ma shows a stronger relationship with the Laiyang Group.

Therefore, in conclusion, we suggest that the Dasheng Group in the Yishu Rift Basin has transitional provenance characteristics from those of the Laiyang Group to the Wangshi Group in the Jiaolai Basin.

5.3 Initial uplift of coastal mountains in the Jiaodong Peninsula

Previous studies have suggested different ages for the initial uplift of coastal mountains. For example, Zhang et al. (2016) and Tan et al. (2020) reported that coastal mountains were uplifted earlier than ~90 Ma on the basis of clumped isotope paleothermometry and provenance analyses in the Jiaolai Basin. He (2022) proposed that there was an uplift event at 110 Ma on the basis of provenance analyses in the Yong'an Basin, south-east China. Chen et al. (2022) reported that coastal mountains began to uplift at ~120 Ma and reached the highest elevation at 90 Ma on the basis of provenance analyses and zircon Eu* anomalies on Hainan Island, south China. Our results suggest that the provenance of the Dasheng Group shows a transitional characteristic from that of the Laiyang Group to that of the Wangshi Group and likely reflects regional paleogeographical changes led by the uplift of the coastal mountains. Therefore, constraining the age of the Dasheng Group is critical since the coastal mountains were initially uplifted during the deposition of the Dasheng Group.

In terms of lithostratigraphy, Liu et al. (2003) indicated that the Dasheng Group generally developed on the top of the Bamudi Formation of the Qingshan Group, and the upper part of the Qingshan Group (the Shiqianzhuang and Fanggezhuang Formations) mostly undeveloped. These authors suggested that the lower part of the Dasheng Group corresponds to the middle-upper part of the Bamudi Formation, whereas its upper part corresponds to the Shiqianzhuang and Fanggezhuang Formations. In terms of biostratigraphy, Si (2002) reported that the spore-pollen assemblages of the Tianjialou and Mengtuan Formations are Schizaeoisporites-Ephedripites-Tricolpites, which are temporally comparable to Cenomanian-Turonian assemblages (~100.5–89.5 Ma). In summary, previous studies suggested that the lower part

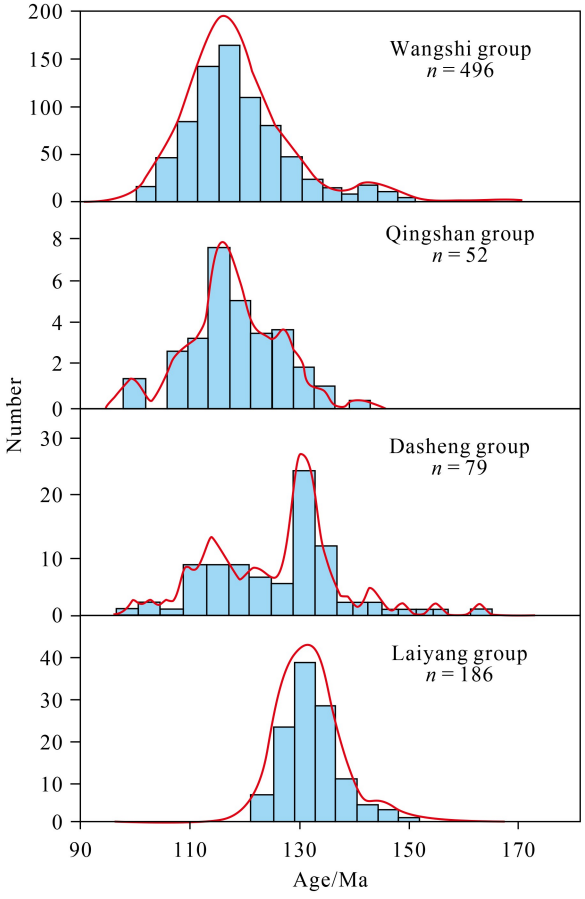

Fig. 7 The Mesozoic zircon age histograms of the Laiyang, Qingshan, Wangshi, and Dasheng groups. The data of the Qingshan Group is derived from An et al. (2016), Cao et al. (2017), and Zhou et al. (2017). The data of the Laiyang Group is derived from Xie et al. (2012) and Wang et al. (2016). The data of the Wangshi Group is derived from Wang et al. (2016) and An et al. (2016). The data of the Dasheng Group is derived from this study.

of the Dasheng Group (i.e., the Malanggou and Tianjialou Formations) is late Early Cretaceous in age, corresponding to the Bamudi, Shiqianzhuang, and Fanggezhuang Formations of the Qingshan Group.

Combining the transitional provenance characteristics of the Dasheng Group, we believe that the initial uplift of the coastal mountains blocked some of the sources from the Sulu Orogenic Belt, and the Jiaobei Terrane during the deposition of the Dasheng Group; thus, the maximum depositional age (MDA) of the Dasheng Group may represent the age of the initial uplift of the coastal mountain. Therefore, we analyze the detrital zircon maximum depositional age (MDA) to further constrain the age of the Dasheng Group (Dickinson and Gehrels, 2009; Coutts et al., 2019). Here, several methods are applied to calculate the MDAs, including the youngest single grain (YSG), youngest graphical peak (YPP), youngest grain cluster (YGC 1σ and YGC 2σ), and youngest detrital zircon (YDZ) methods. The calculations are as follows. 1) YSG: the youngest single DZ grain age

with 1σ uncertainty from a table of U-Pb grain ages, except that where 1σ > 10 Ma for the youngest single grain age and where the grain age overlaps at 1σ with the next youngest grain age, the latter grain age is substituted for greater precision (Dickinson and Gehrels, 2009). 2) YPP: the youngest graphical DZ age peak on an age-probability plot or age-distribution curve, as controlled by multiple U-Pb grain ages (single-grain age peaks ignored). YPP incorporates at least minimal reproducibility as a measure of the youngest DZ age, can be determined from published age–distribution curves without ready access to tables of U-Pb grain ages, and honors the perspective that grain ages plotting on the shoulders of age peaks may be just a reflection of analytical imprecision (Dickinson and Gehrels, 2009). For improved resolution, YPP ages were picked from the crests of the youngest discrete age peaks visible on age-distribution curves via expanded abscissas of Excel graphs generated by Isoplot (Ludwig, 2008). (3) YGC 1σ (2 +): weighted mean age (± 1σ incorporating both internal analytical error and external systematic error) of the youngest cluster of two or more grain ages ($n \geqslant 2$) overlapping in age at 1σ. (4) YGC 2σ (3 +): weighted mean age (± 1σ incorporating both internal analytical error and external systematic error) of the youngest cluster of three or more grain ages ($n \geqslant 3$) overlapping in age at 2σ. YGC 2σ (3 +) provides a more statistically robust and conservative measure of the youngest DZ age than does YGC 1σ (2 +) (Dickinson and Gehrels, 2009). (5) YDZ: age calculated via the "Youngest Detrital Zircon" routine of Isoplot (Ludwig, 2008). YDZ is generated via a Monte Carlo analysis on the basis of the youngest subset of DZ ages in a DZ population. In general, the plus and minus uncertainties for the resultant YDZ are unequal (Dickinson and Gehrels, 2009).

Our analyses yield the following ages: YSG at 99 Ma, YPP at 127 Ma, YGC 1σ at 99.5 Ma, YGC 2σ at 98.7 Ma, and YDZ at 96.875 +2/−4.6 Ma. After excluding the YPP age due to the large deviation, we suggest that the MDAs range from 99.5 to 96.5 Ma and suggest that the Dasheng Group was less than 100 Ma in age. Recently, many geochronological studies have suggested that the Dasheng Group is Aptian–Albian in age. For example, Tang et al. (2008) dated the tuffs in the Tianjialou Formation to 95 Ma, Li et al. (2012) dated the subvolcanic rocks in the Dasheng Group to 96.5 Ma, and Xu et al. (2017) dated the explosive-overflow breccia and coarse andesite between the Tianjialou and Hongtuya Formations to 99.5 Ma. These ages align with our MDAs and support a depositional age of ~100 Ma for both the lower part of the Dasheng Group and the initial uplift of the coastal mountains in the Jiaodong Peninsula.

5.4 Cretaceous paleogeographic evolution of the Jiaodong Peninsula

During the Early Cretaceous, east China experienced an extensional tectonic regime. Since the coastal mountains had not yet uplifted, both the Jiaolai Basin and the Yishu Rift Basin had relatively low altitudes during this period (Fig. 8(a)). Their sedimentary provenance characteristics are so consistent that they may reflect material exchange between these two paleolakes, and we speculate that the Jiaolai Basin and Yishu Rift Basin may have connected to form a large lake during the Early Cretaceous. The paleocurrents mainly originated from the SW and SE directions during this period (Yu et al., 2003). The Sulu Orogenic Belt and Jiaobei Terrane provide the main sediments for these two basins. In addition, the Luxi Uplift also provided sediments to the Yishu Rift Basin

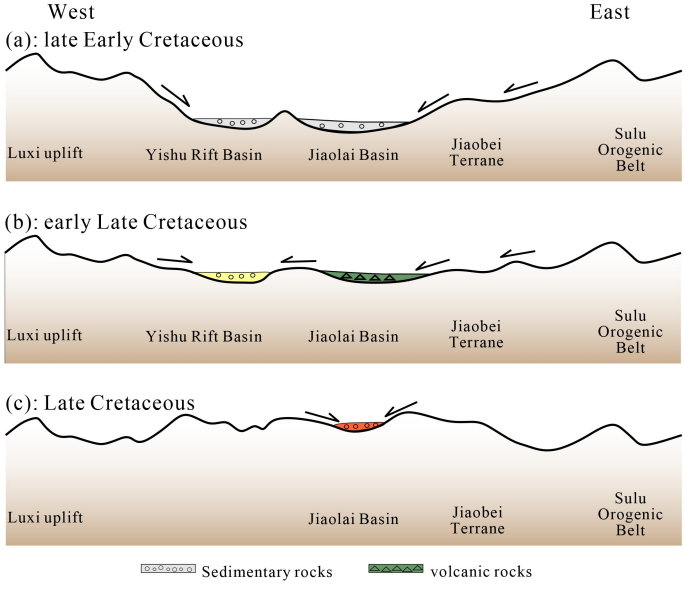

Fig. 8 The sketch map of the Yishu Rift Basin and the Jiaolai Basin during the Cretaceous (not to scale).

(Bu et al., 2012). The vegetation in the Jiaodong Peninsula were broad-leaved evergreen forests (Liu et al., 2011), the lakes were developed with rivers, and the paleoclimate was warm and humid (Zhang et al., 2016).

During the late Early Cretaceous to early Late Cretaceous, the extensional tectonic regime in east China switched to a compressional tectonic regime, possibly caused by paleo-Pacific plate subduction or the Okhotomorsk Block collision at ~100 Ma (Yang, 2013; Zhang et al., 2016). The coastal mountains initially uplifted, but their paleoelevation was relatively low and had only minimal influence on the basin provenances (Fig. 8(b)). During this period, intense volcanic activity occurred in the Jiaolai Basin (Liu et al., 2003; Song, 2020; Tan et al., 2020). In addition, clasts from the Luxi Uplift, Yishu Rift Basin, also received limited provenances from its surrounding area. Compared with the warm and humid paleoclimate during the Early Cretaceous, multiple dry–wet cycles may have been influenced by the initial uplift of coastal mountains during the late Early Cretaceous to the early Late Cretaceous (Li and Zhao, 1992; Liu et al., 2003).

During the Late Cretaceous, the coastal mountains uplifted significantly. On the basis of clumped isotope paleothermometry, Zhang et al. (2016) suggested that the paleo-elevation of coastal mountains was greater than 2 km at ~80 Ma. During this period, the Yishu Rift Basin shrank and disappeared, and the Jiaolai Basin was uplifted into an intermontane basin (Fig. 8(c)). The sediment transport into the Jiaolai Basin was blocked by the coastal mountains and left only limited materials from the basin margins (Tan et al., 2020). During the Late Cretaceous, the Jiaolai Basin experienced relatively poor hydrological conditions, and the paleoclimate was relatively arid, which is also supported by extensive red-colored alluvial fan deposits and paleosol carbonates and the burial of massive dinosaur fossils by large-scale mud flow deposits in the Jiaolai Basin during the Late Cretaceous (Cao, 2013; Liu et al., 2015; Wang, 2019).

6 Conclusions

In this study, we investigate the Cretaceous provenance evolution of the Dasheng Group in the Yishu Rift Basin, east China, and its implications for the uplift of the coastal mountains. The conclusions are as follows.

1) The age peaks of the Dasheng Group include 2500–2300 Ma, 1850–1600 Ma, 800–500 Ma, 330–215 Ma, and 150–122 Ma, with the highest peak occurring at 150–122 Ma, followed by 1850–1600 Ma. After comparison with the surrounding source area, we infer that the provenance of the Dasheng Group was mainly the Luxi Uplift, the Sulu Orogenic Belt, and the Jiaobei Terrane.

2) Compared with those of the Jiaolai Basin, the zircon age peaks of the Dasheng Group in the Yishu Rift Basin are nearly the same as those of the Lower Cretaceous Laiyang Group, but the proportion of pre-Mesozoic zircons decreases. For the Dasheng Group, there are two zircon age peaks with Mesozoic ages, and the main peak corresponds to the Laiyang Group, whereas the secondary peak corresponds to the Wangshi Group. Therefore, we suggest that the provenance of the Dasheng Group has transitional characteristics from that of the Laiyang Group to that of the Wangshi Group in the Jiaolai Basin.

3) During the Early Cretaceous, the Jiaolai Basin and the Yishu Rift Basin may have connected to form a large lake and received provenances from the Sulu Orogenic Belt, Jiaobei Terrane, and Luxi Uplift. During the late Early Cretaceous to early Late Cretaceous, the coastal mountains initially uplifted but their paleoelevation was relatively low and had only minimal influence on the basin provenances. During the Late Cretaceous, the coastal mountains continued to rise. The Yishu Rift Basin shrank and disappeared and the Jiaolai Basin was uplifted into an intermontane basin. The sediment transport into the Jiaolai Basin was blocked by the coastal mountains and left only limited materials from the basin margins.

Acknowledgments This study was financially supported by the National Key R&D Plan of China (No. 2023YFF0803303), the National Natural Science Foundation of China (Grant No. 42072116), and the Fundamental Research Funds for the Central Universities (No. 2652023001 and **265202103).**

Competing interests The authors declare that they have no competing interests.

References

An W, Kuang H W, Liu Y Q, Peng N, Xu K M, Xu H, Zhang P, Wang K B, Chen S Q, Zhang Y X (2016). Detrital zircon dating and tracing the provenance of dinosaur bone beds from the Late Cretaceous Wangshi Group in Zhucheng, Shandong, east China. J Palaeogeogr, 5(1): 72–99

Bu X P, Shi Y H, Li Z (2012). Heavy minerals assemblage analysis and its structural indication in Late Mesozoic basin of Luxi uplift. Chin J Geo, 47(4): 1116–1129 (in Chinese)

Cao G, Xue H, Liu Z (2017). Latest zircon U-Pb geochronology of the Qingshan groupvolcanic rocks along the Tan–Lu fault zone of Shandong Province, eastern China. Acta Geol Sin, 91: 2333–2335

Cao K (2013). Cretaceous terrestrial stratigraphic correlation in China. Geol Rev, 59: 24–40 (in Chinese)

Cao S, Zhang L, Mountney N P, Ma J, Hao M, Wang C (2023). Ultra-long-distance transport of aeolian sand: the provenance of an intermontane desert, south-east China. Sedimentology, 70(7): 2108–2126

Cao S, Zhang L, Wang C, Ma J, Tan J, Zhang Z (2020). Sedimentological characteristics and aeolian architecture of a plausible intermountain erg system in southeast China during the Late Cretaceous. Geol Soc Am Bull, 132(11–12): 2475–2488

Chen P (1997). Coastal mountains of SE China, desertization and saliniferous lakes of central China during the Upper Cretaceous. J Stratigrapgh, 21(3): 203–213 (in Chinese)

Chen Y, Meng J, Liu H, Wang C, Tang M, Liu T, Zhao Y (2022). Detrital zircons record the evolution of the Cathaysian Coastal Mountains along the south China margin. Basin Res, 34(2): 688–701

Coutts D S, Matthews W A, Hubbard S M (2019). Assessment of widely used methods to derive depositional ages from detrital zircon populations. Geosci Front, 10(4): 1421–1435

Dickinson W R, Gehrels G E (2009). Use of U-Pb ages of detrital zircons to infer maximum depositional ages of strata: a test against a Colorado Plateau Mesozoic database. Earth Planet Sci Lett, 288(1–2): 115–125

Geisler T, Rashwan A A, Rahn M K W, Poller U, Zwingmann H, Pidgeon R T, Schleicher H, Tomaschek F (2003). Low–temperature hydrothermal alteration of natural metamict zircons from the Eastern Desert, Egypt. Mineral Mag, 67(3): 485–508

Geisler T, Ulonska M, Schleicher H, Pidgeon R T, van Bronswijk W (2001). Leaching and differential recrystallization of metamict zircon under experimental hydrothermal conditions. Contrib Mineral Petrol, 141(1): 53–65

Guo P (2014). Geodynamic setting of Mesozoic gold metallogeny in the western Shandong Province. Dissertation for Doctoral Degree. Beijing: China University of Geosciences (Beijing)

He A B (2022). Evolution of Paleo–coastal mountains along the southeast coast: sedimentation and paleoclimate response in Yong' an Basin of the late Mesozoic. Dissertation for Doctoral Degree. Beijing: University of Chinese Academy of Sciences

Hermann J, Rubatto D, Korsakov A, Shatsky V S (2001). Multiple zircon growth during fast exhumation of diamondiferous, deeply subducted continental crust (Kokchetav Massif, Kazakhstan). Contrib Mineral Petrol, 141(1): 66–82

Hoskin P W, Schaltegger U (2003). The composition of zircon and igneous and metamorphic petrogenesis. Rev Mineral Geochem, 53(1): 27–62

Hou G, Liu Y, Li J, Jin A (2005). The SHRIMP U-Pb chronology of mafic dyke swarms: a case study of Laiwu diabase dykes in western Shandong. Acta Petrol et Mineral, 24(3): 179–185 (in Chinese)

Hu G, Hu W, Cao J, Yao S, Xie X, Li Y, Liu Y, Wang X (2012). Deciphering the Early Cretaceous transgression in coastal southeastern China: constraints based on petrography, paleontology and geochemistry. Palaeogeogr Palaeoclimatol Palaeoecol, 317–318: 182–195

Hu Q, Li L, Tang Z, Shi X (2009). Characteristics and mechanism of Late Mesozoic extensional faults in West Shandong Uplift. Geo China, 36(6): 1233–1244 (in Chinese)

Jiang X, Pan Z, Xu J, Li X, Xie J, Xiao Z (2006). Late Cretaceous eolian dunes and wind directions in Xinjiang basin, Jiangxi Province, China. Geol Bull China, 25(7): 833–838 (in Chinese)

Kerrich R, King R (1993). Hydrothermal zircon and baddeleyite in Val–d'Or Archean mesothermal gold deposits: characteristics, compositions, and fluid–inclusion properties, with implications fortiming of primary gold mineralization. Can J Earth Sci, 30(12): 2334–2351

Li C M (2009). A review on the minerageny and situ microanalytical dating techniques of zircons. Geol Survey Res, 33(3): 161–174 (in Chinese)

Li Q P, Zhao J F (1992). Establishment and time correlation of the Dasheng Group of the lower cretaceous series in Shandong. Geo Shandong, 8(2): 13–21 (in Chinese)

Li S, Wang J, Liu J, Yu J, Lu H, Hou F (2005). Mesozoic structure and its tectonic setting in the western Shandong block. Acta Geol Sin–Chin Ed, 79(4): 487–497 (in Chinese)

Li X H, Chen F, Guo J H, Li Q L, Xie L W, Siebel W (2007). South China provenance of the lower–grade Penglai Group north of the Sulu UHP orogenic belt, eastern China: evidence from detrital zircon ages and Nd–Hf isotopic composition. Geochem J, 41(1): 29–45

Li Y L, Qiu J S, Liu L (2012). Geochronology and geochemistry of sodic volcanic rocks from Shenquan in Tancheng County Shandong Province: implications for unraveling the nature of mantle source and petrogenesis. Acta Petrol Mineral, 31(6): 783–798 (in Chinese)

Liu J, Liu F, Ding Z, Liu C, Yang H, Liu P, Wang F, Meng E (2013a). The growth, reworking and metamorphism of early Precambrian crust in the Jiaobei terrane, the North China Craton: constraints from U–Th–Pb and Lu–Hf isotopic systematics, and REE concentrations of zircon from Archean granitoid gneisses. Precambrian Res, 224: 287–303

Liu J, Liu F, Ding Z, Yang H, Liu C, Liu P, Xiao L, Zhao L, Geng J (2013b). U-Pb dating and Hf isotope study of detrital zircons from the Zhifu Group, Jiaobei Terrane, North China Craton: provenance and implications for Precambrian crustal growth and recycling. Precambrian Res, 235: 230–250

Liu M W, Zhang Q Y, Song W Q (2003). Division of the Cretaceous lithostratigraphic and volcanic sequences of Shandong. J Stratigrapgh, 27(3): 247–253 (in Chinese)

Liu P, Liu F, Yang H, Wang F, Liu J (2012). Protolith ages and timing of peak and retrograde metamorphism of the high–pressure granulites in the Shandong Peninsula, eastern North China Craton. Geosci Frontier, 3(6): 923–943

Liu S Y (2018). Petrogenesis and magma source of the Mesozoic complexes in western Shandong Province. Dissertation for Master's Degree. Beijing: China University of Geosciences (Beijing), 1–72 (in Chinese)

Liu S, Zhang B, Ma P, Williams S, Lin C, Wan N, Ran C, Gurnis M (2024). Craton deformation from flat–slab subduction and rollback. Nat Geosci, 17(9): 936–943

Liu Y Q, Kuang H W, Peng N, Ji S A, Wang X R, Chen S Q, Zhang Y X, Xu H (2010a). Sedimentary facies and taphonomy of Late Cretaceous deaths of dinosaur, Zhucheng, eastern Shandong. Geol Rev, 56(4): 457–468 (in Chinese)

Liu Y Q, Kuang H W, Peng N, Xu H, Liu Y X (2011). Sedimentary facies of dinosaur trackways and bonebeds in the Cretaceous Jiaolai Basin, eastern Shandong, China, and their paleogeographical implications. Earth Sci Front, 18(4): 9–24

Liu Y Q, Kuang H W, Peng N, Xu H, Zhang P, Wang N S, An W, Wang Y, Liu M, Hu X F (2015). Mesozoic basins and associated palaeogeographic evolution in North China. J Palaeogeogr, 4(2): 189–202

Liu Y S, Gao S, Hu Z C, Gao C G, Zong K Q, Wang D B (2010b). Continental and oceanic crust recycling–induced melt–peridotite interactions in the Trans–North China Orogen: U-Pb dating, Hf isotopes and trace elements in zircons from mantle xenoliths. J Petrol, 51(1–2): 537–571

Ludwig K R (2008). Isoplot 3.6: a geochronological toolkit for Microsoft Excel. Berkeley Geochronology Center Special Publication, 4: 1

Luo W Q, Zhang S K, Yu X F, Tian J X, Yang B, Zhang Y, Chen J, Ma X X, Tang, L L, Sun X Z (2018). Review on research progress of Yishu fault zone. Shandong Land Resour, 59–65 (in Chinese)

Morton A C, Hallsworth C (1994). Identifying provenance–specific features of detrital heavy mineral assemblages in sandstones. Sediment Geol, 90(3−4): 241–256

Pidgeon R T, Nemchin A A, Hitchen G J (1998). Internal structures of zircons from Archaean granites from the Darling Range batholith: implications for zircon stability and the interpretation of zircon U-Pb ages. Contribut Mineral Petrol, 132(3): 288–299

Si S Y (2002). Palynological assemblage from the Dasheng Group and its significance in Shandong Province. J Stratigraph, 26(2): 126–130 (in Chinese)

Song L G (2020). Geochemical Characteristics and Pronvence of Sandstone of Dasheng Group Malanggou Formation in the Mid–part of the Yishu Fault Zone, Shandong Province, China. Dissertation for Master's Degree. Qingdao: Shandong University of Science and Technology

Song M C, Li H K (2001). Study on regional geological structural evolution in Shandong Province. Geo Shandong, 17(6): 12–21 (in Chinese)

Suo Y, Li S, Jin C, Zhang Y, Zhou J, Li X, Wang P, Liu Z, Wang X, Somerville I (2019). Eastward tectonic migration and transition of the Jurassic–Cretaceous Andean–type continental margin along southeast China. Earth Sci Rev, 196: 102884

Tan J, Zhang L, Wang C, Cao K, Li X (2020). Late cretaceous provenance change in the Jiaolai Basin, east China: implications for paleogeographic evolution of East Asia. J Asian Earth Sci, 194: 104188

Tang J, Liu T, Wang Q (2008). Geochoromlogy of Mesozoic volcanic rocks in Shandong province. Acta Petrol Sin, 24(6): 1333–1338 (in Chinese)

Tang J, Zheng Y F, Wu Y B, Gong B, Liu X (2007). Geochronology and geochemistry of metamorphic rocks in the Jiaobei terrane: constraints on its tectonic affinity in the Sulu orogen. Precambrian Res, 152(1–2): 48–82

Torres L, Olivar G, Casanova S (2012). Bifurcations in a Generalization of the ZAD Technique: application to a DC-DC Buck Power Converter. Math Probl Eng, 2012(1): 520296

Wang J, Chang S C, Lu H B, Zhang H C (2016). Detrital zircon provenance of the Wangshi and Laiyang groups of the Jiaolai basin: evidence for Early Cretaceous uplift of the Sulu orogen, eastern China. Int Geol Rev, 58(6): 719–736

Wang P (1998). Deformation of Asia and global cooling: searching links between climate and tectonics. Quat Sci, 18(3): 213–221 (in Chinese)

Wang P (2004). Cenozoic deformation and the history of sea–land interactions in Asia. Geophys Monogr, 149: 1–22

Wang Y J (2019). Formation in the Guangfeng Basin of Jiangxi Province Sedimentary Characteristics and Paleoclimate of the Zhoutian. Dissertation for Master's Degree. Nanchang: East China University of Technology

Wiedenbeck M (1995). An example of reverse discordance during ion microprobe zircon dating: an artifact of enhanced ion yields from a radiogenic labile Pb. Chem Geol, 125(3–4): 197–218

Woodhead J D, Hellstrom J, Hergt J M, Greig A, Maas R (2007). Isotopic and elemental imaging of geological materials by laser ablation inductively coupled plasma‐mass spectrometry. Geostand Geoanal Res, 31(4): 331–343

Woodhead J, Hergt J, Shelley M, Eggins S, Kemp R (2004). Zircon Hf–isotope analysis with an excimer laser, depth profiling, ablation of complex geometries, and concomitant age estimation. Chem Geol, 209(1–2): 121–135

Wu C, Rodriguez–Lopez J P, Santosh M (2022). Plateau archives of lithosphere dynamics, cryosphere and paleoclimate: the formation of Cretaceous desert basins in east Asia. Geosci Front, 13(6): 101454

Wu M, Zhao G, Sun M, Li S, Bao Z, Tam P Y, Eizenhöefer P R, He Y (2014). Zircon U-Pb geochronology and Hf isotopes of major lithologies from the Jiaodong Terrane: implications for the crustal evolution of the Eastern Block of the North China Craton. Lithos, 190–191: 71–84

Wu Y B, Zheng Y F, Zhou J B (2004). Neoproterozoic granitoid in northwest Sulu and its bearing on the North China‐South China Blocks boundary in east China. Geophys Res Lett, 31(7): L07616

Wu Y, Zheng Y (2013). Tectonic evolution of a composite collision orogen: an overview on the Qinling–Tongbai Hong'an–Dabie–Sulu orogenic belt in central China. Gondwana Res, 23(4): 1402–1428

Xie S, Wu Y, Zhang Z, Qin Y, Liu X, Wang H, Qin Z, Liu Q, Yang S (2012). U-Pb ages and trace elements of detrital zircons from Early Cretaceous sedimentary rocks in the Jiaolai Basin, north margin of the Sulu UHP terrane: provenances and tectonic implications. Lithos, 154: 346–360

Xu J Q, Li Z, Shi Y H (2012). Major provenance of Jurassic sediments in Luxi uplift, eastern north China, derived from the northern north China Block: evidences from detrital zircon U-Pb and Hf isotopic geochronology. Chin J Geo, 47(4): 1099–1115 (in Chinese)

Xu K M, Qin J, Wang Y P (2017). Research Progress on Fine Rock Stratigraphic Framework and Chronostratigraphic Framework in Jiaolai Basin, Shandong Province. In: Annual Meeting of Chinese Geoscience Union

Yan Y, Hu X Q, Lin G, Santosh M, Chan L S (2011). Sedimentary provenance of the Hengyang and Mayang basins, SE China, and implications for the Mesozoic topographic change in South China Craton: evidence from detrital zircon geochronology. J Asian Earth Sci, 41(6): 494–503

Yang F, Santosh M, Glorie S, Jepson G, Xue F, Kim S W (2020). Meso–Cenozoic multiple exhumation in the Shandong Peninsula, eastern North China Craton: implications for lithospheric destruction. Lithos, 370–371: 105597

Yang Y T (2013). An unrecognized major collision of the Okhotomorsk Block with East Asia during the Late Cretaceous,

constraints on the plate reorganization of the Northwest Pacific. Earth Sci Rev, 126: 96–115

Yu F S, Qi J F, Wang C Y (2003). Analysis of origin of the Early Cretaceous Dasheng–Mazhan Basin in the North Part of Yi–shu fracture. J Xi'an Petrol Institute, 18(1): 1–3 (in Chinese)

Zhang B, Liu S, Lin C, Wang Y, Wang Z, Fang M, Shen W (2019). Source–to–sink system reconstruction in the northern Jiaolai Basin, eastern China, by multiproxy provenance methods and implications for exhumation of the Sulu orogen. Tectonophysics, 754: 18–32

Zhang B, Liu S, Lin C, Wang Y, Wang Z, Fang M, Shen W (2021a). Provenance of the Late Cretaceous sediments in Jiaolai Basin, eastern China, and its tectonic implications. Int Geol Rev, 63(8): 973–991

Zhang J, Liu Y, Flögel S, Zhang T, Wang C, Fang X (2021b). Altitude of the East Asian coastal mountains and their influence on Asian climate during early Late Cretaceous. J Geophys Res: Atmos, 126(22): e2020JD034413

Zhang J, Zhao Z F, Zheng Y F, Dai M (2010). Postcollisional magmatism: geochemical constraints on the petrogenesis of Mesozoic granitoids in the Sulu orogen, China. Lithos, 119(3–4): 512–536

Zhang L, Wang C, Cao K, Wang Q, Tan J, Gao Y (2016). High elevation of Jiaolai Basin during the Late Cretaceous: implication for the coastal mountains along the East Asian margin. Earth Planet Sci Lett, 456: 112–123

Zhang X, Pease V, Omma J, Benedictus A (2015). Provenance of Late Carboniferous to Jurassic sandstones for southern Taimyr, Arctic Russia: a comparison of heavy mineral analysis by optical and QEMSCAN methods. Sediment Geol, 329: 166–176

Zhang Y Q, Li J L, Zhang T, Dong S W, Yuan J Y (2008). Cretaceous to Paleocene tectono–sedimentary evolution of the Jiaolai Basin and the contiguous areas of the Shandong Peninsula (north China) and its geodynamic implications. Acta Geol Sin, 82(9): 1229–1257 (in Chinese)

Zhang Y, Dong S (2008). Mesozoic tectonic evolution history of the Tan–Lu fault zone: advances and new understanding. Geol Bull China, 27(9): 1371–1390 (in Chinese)

Zhao R, Wang Q F, Liu X F, Wang W, Pan R G (2016). Architecture of the Sulu crustal suture between the North China Craton and Yangtze Craton: constraints from Mesozoic granitoids. Lithos, 266–267: 348–361

Zhou J B, Wilde S A, Zhao G C, Zheng C Q, Jin W, Zhang X Z, Cheng H (2008). SHRIMP U-Pb zircon dating of the Neoproterozoic Penglai Group and Archean gneisses from the Jiaobei Terrane, north China, and their tectonic implications. Precambrian Res, 160(3–4): 323–340

Zhou Y Q, Peng T M, Zhou T F, Zhang Z K, Tian H, Liang W D, Yu T, Sun L F (2017). Soft–sediment deformation structures related to volcanic earthquakes of the lower Cretaceous Qingshan group in Lingshan Island, Shandong Province, east China. J Palaeogeogr, 6(2): 162–181